Design and Analysis of RFID Reader antenna for UHF Near field Applications

[1]B.RamaGopi, [2]D.Jagadeesh
[1]Student of M.Tech, [2]Assistant Professor
[1]Department of ECE,
[1]RVR & JC College of Engineering,Guntur, India

Abstract: **This paper presents an ultrahigh frequency (UHF) radio frequency identification (RFID) reader antenna used to detect an RFID tag. The antenna works in the UHF range i.e., 860-960 MHz, and also it is easy to design and low cost. A 90° phase shift is introduced between the currents flowing along the opposite side of two branches, this results in the near-field and multi-polarization operation. The simulated impedance bandwidths (−10 dB) range from 825 to 965 MHz and covering the UHF RFID standard. In addition, it exhibits a high far-field gain. The large dimensions of the antenna contributed to the high far-field gain of 23.45 dB and directivity of 19.9 dB. Thus the simulated results of the antenna are in good agreement with the specified UHF band and ranges.**

***IndexTerms*– Multi-polarization, near-field application, radio frequency identification (RFID), reader antenna, ultrahighfrequency(UHF).**

I. INTRODUCTION

RFID technology is used to provide wireless identification and tracking capability [1][2], it is developed around World War II. Radio Frequency Identification (RFID) Systems enable the user to simultaneously read/write the tags and activate remote sensing devices based on their unique IDs [3]. Near-field RFID readers are becoming more and more prominent due to the item-level RFID applications like as sensitive products tracking, pharmaceutical logistics, transport, medical products, and bio-sensing applications [4]–[8].In most of the near-field RFID applications, the interaction between tags and the reader antennas is based on magnetic coupling, whose magnetic field stores most of the reactive energy. Usually, the general electrically small loops can produce a strong magnetic field over the near-field region. The main challenge encountered in designing the reader Antenna is to generate a strong and uniform magnetic-field distribution over an electrically large interrogation zone area using one single antenna. On the other hand, a large interrogation zone of the reader antenna is able to detect more tags simultaneously and make an RFID system more efficient. This near-field magnetic field can also be generated by the interference between the feed line and the meander line [9]. These magnetic coupling-based antennas can detect a large number of loop-like tags, but their short reading distance limits the scope of their applications. In this paper, we have proposed and investigated a novel UHF RFID reader antenna with high far-field gain and also multi-polarization operations. The proposed antenna is low in cost and easy to fabricate. The antenna comprises two meandering open-ended microstrip lines and a phase shifter of approximately 90°. The simulated -10dB impedance bandwidth of the antenna ranges from 825 to 965 MHz, which covers all the UHF RFID standards.

II. Antenna design and configuration

A. Antenna Configuration

The configuration of the proposed antenna is shown in Fig. 1. The antenna comprises a pair of open-ended symmetrical microstrip meandering lines with a phase shifter in one branch. The antenna prototype was fabricated on a 1-mm-thick FR4 substrate with a permittivity of 4.4, a length (L) of 255.6 mm, and a width (W) of 220 mm. The bottom of the substrate was on a covered metal ground. On the input side, the antenna was fed by a 50- Subminiature version A connector. The matching stub is used to match the input impedance and divide the electromagnetic energy uniformly into two branches. The optimized dimensions of the antenna are presented in Table I. The operation of the antenna will be explained in the following sections.

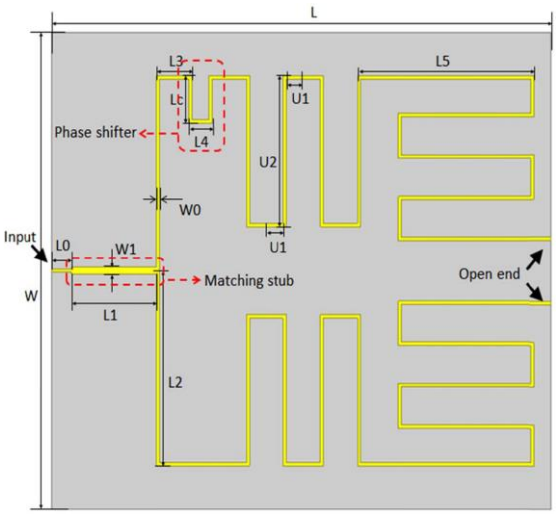

Fig. 1. Configuration of the proposed antenna

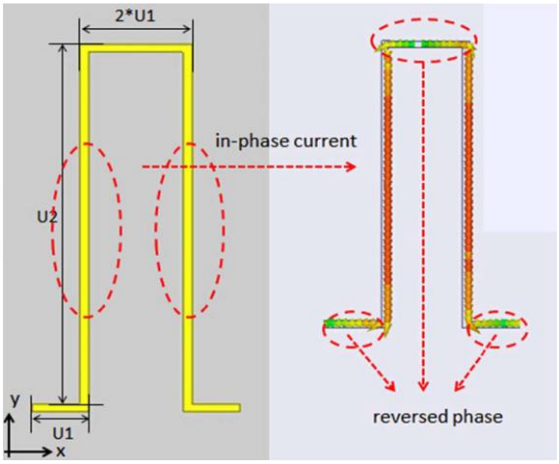

Fig. 2. Meander unit and the simulated current distribution

B. Introduction of Microstrip Meander Units

To explain the operating principle of the proposed antenna, a simplified structure of the meander unit is analyzed, as shown in Fig. 2. The segments U1 and U2 satisfy the following equation:

$4 \times U1 + 2 \times U2 = \lambda g(1)$

Where λgis the operating on-board wavelength.

W0	W1	U1	U2	L0	L1	L2	L3	L4	L6	Lc
1.6mm	3mm	8.7mm	69.7mm	10mm	43.6mm	90mm	18.2mm	11.9mm	88.7mm	22mm

Table I: Dimensions Of Optimized Antenna Design

The proposed antenna comprises eight differently oriented units, the length of each unit being equal to one operating wavelength. Owing to the open end, the standing wave can be formed on the meandered lines to generate a strong electric field in the near-field region. The distribution of electric current flowing along the lines and the locations of nodes can be easily adjusted by changing the lengths of *U*1 and *U*2. As shown in the simulation results (Fig. 2), the antinodes, i.e., the maximum electric current amplitude, were moved to the middle part of *U*2. The electric currents along *U*2 segments are in-phase and superposed to enhance the strength of the electric field.

The currents along the *y*-axis create a strong E-field in the central region above the unit, but those along *U*1 segments are too weak to excite the electric field. Fig. 3 illustrates the distribution of simulated E-field vectors within a cycle on a plane at distance of 300 mm from above the unit. It is shown that the E-field vectors in the *xoy*plane are predominately along *y*-axis.

C. Principle of Multipolarization

The proposed antenna comprises a pair of symmetrical branches of differently oriented (vertical and horizontal) units plus a phase shifter in the upper branch. The phase shifter consists of two *Lc*stubs with a total length being approximately equal to a quarter of the operating wavelength.So the phase shifter causes a phase difference of 90° between the upper and lower branches. Fig. depicts the current distributions in the antenna structure in four different phases over a cycle. It can be seen that the current direction is changed with the phase. In the phase of 0°, the horizontal currents on the units of upper and lower branches flow in the opposite direction while the currents flow in the same upward direction on the vertical units. Therefore, the horizontal currents cancel themselves out while the vertical currents are enhanced in the upward direction. In the phase of 90°, the vertical currents on the upper and lower branches flow in the opposite direction and cancel themselves out while the horizontal currents are enhanced in the same rightward direction. In the phase of 180°, the horizontal currents cancel themselves out again while the vertical currents are enhanced in the

downward direction. In the phase of 270°, the vertical currents cancel themselves out while the horizontal currents are enhanced in the leftward direction. Therefore, the 90° phase difference between the upper branch and the lower branch has generated a quasi-circular polarization of the enhanced current on this antenna. In addition, a quarter-wavelength match stub from 50 to 25 is inserted in the feeding end to divide the electromagnetic power uniformly into the two branches. The matching stub is designed with a length L1 = 43.6 mm and a width W1 = 3 mm. Fig. 5 presents the simulated E-field vector distributions in the corresponding phases of Fig. 4 on the xy plane 300 mm above the antenna surface. The directions of E-field vectors match the directions of the enhanced currents in Fig. 4 perfectly, following a similar quasi-circular polarization. Thus, the arbitrarily oriented linear-polarized tags can be detected in the near field of antenna.

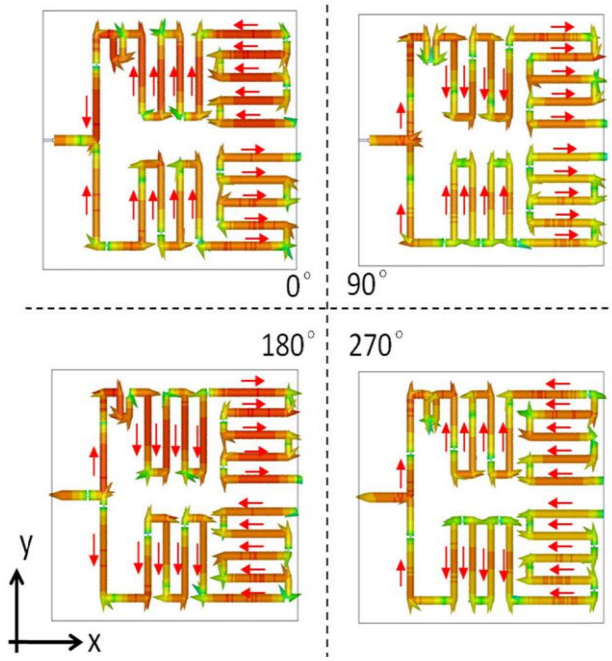

Fig. 3. Current distributions in the antenna structure over a cycle

.For better understanding of the antenna operation, the E-field vector distributions in the same horizontal plane, but without the phase shifter in the upper branch. It can be seen that the directions of E-field vectors are alternate only along the *x*-axis over a cycle. The linear-polarized tags along the *y*-axis cannot be detected in this plane . Distribution of electric field vectors at.
In the plane close to the antenna, the directions of the E-field vectors are in mixed orientation, as shown in Fig. . So the arbitrarily oriented linearly polarized tags on this plane can be detected. Thus, the direction of the E-field vectors of the proposed antenna presents the multi polarized characteristic on the plane parallel to the antenna.

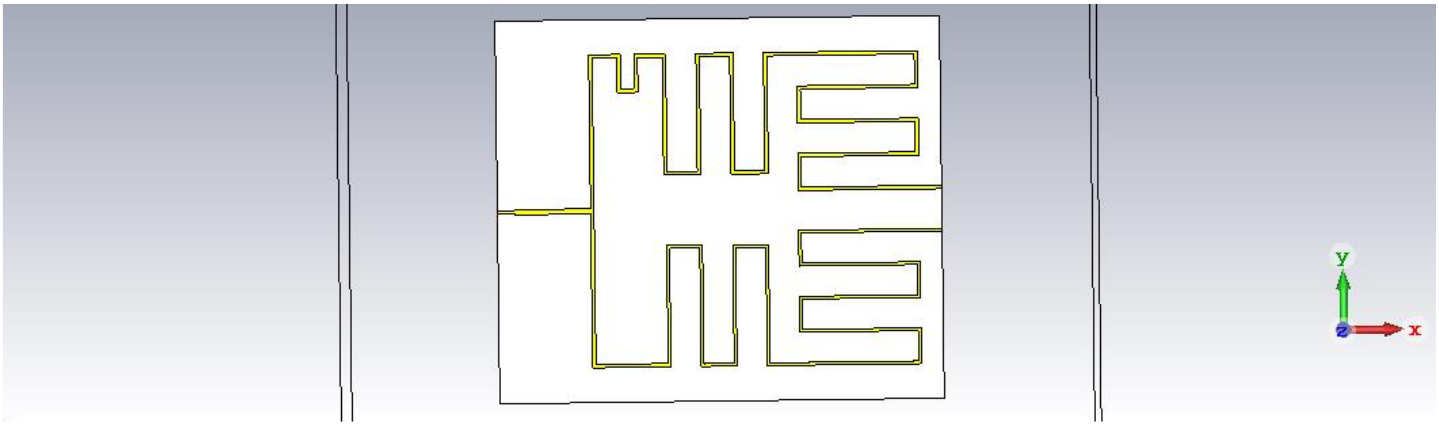

Figure. 4 : Design of Proposed antenna.

III. Stimulation Results

Return loss:

The simulated return loss of antenna is shown in figure

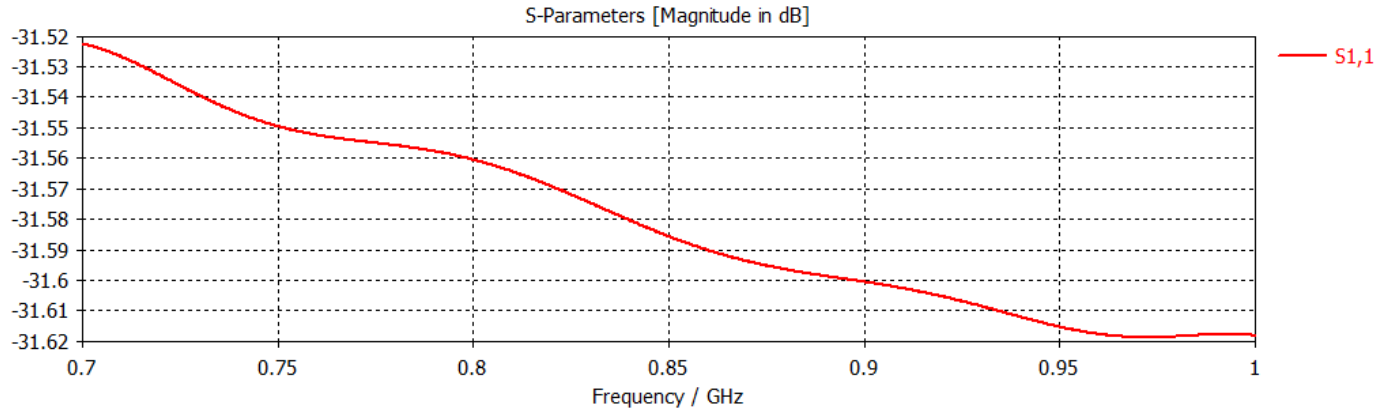

Figure. 5 : Return loss plot of Proposed antenna

VSWR:

The Simulated VSWR is below -10 dB level.VSWR stands for Voltage Standing Wave Ratio. VSWR is a function of the reflec- tion coefficient, which describes the power reflected from the antenna. The smaller the VSWR is, the better antenna is matched to the transmission line and more power is de- livered to the antenna.

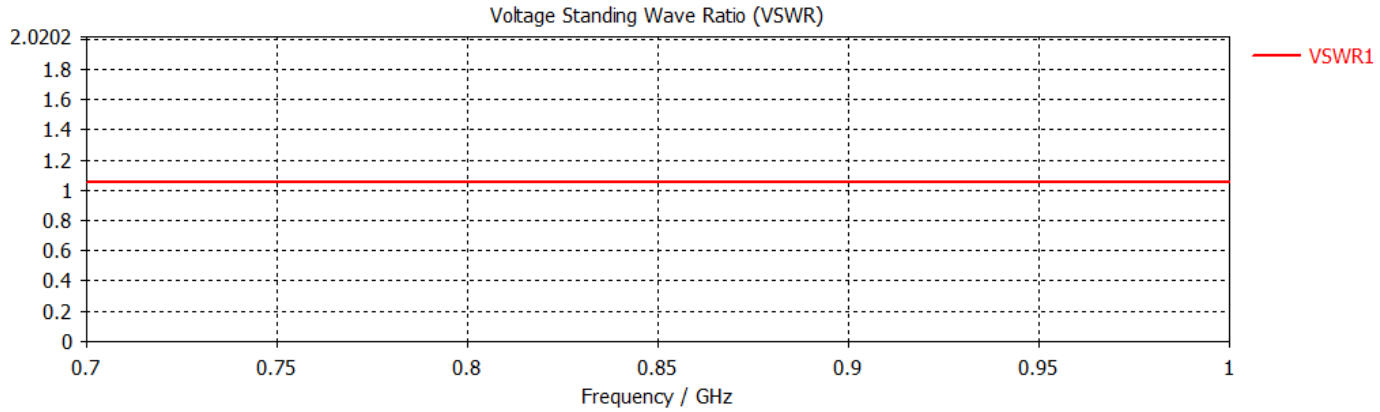

Figure.6 : Voltage Standing Wave Ratio plot of Proposed Patch antenna.

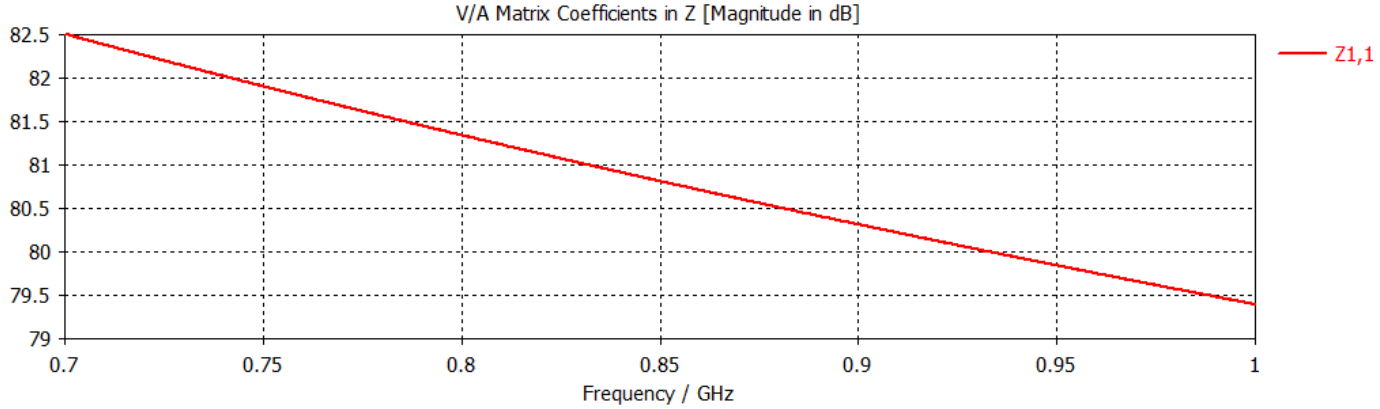

Figure .7: Impedance of Proposed Patch antenna

Radiation Patterns:

The radiation pattern is a graphical depiction of the relative field strength transmitted from or received by the antenna. The antennas patterns describes how the antenna radiates energy out into space. An antenna radiates energy in all directions, at least to some extent. So, the antenna pattern is actually three dimensional. The far field radiation patterns in terms of 3D view for the proposed Microstrip antenna are shown in
below figures

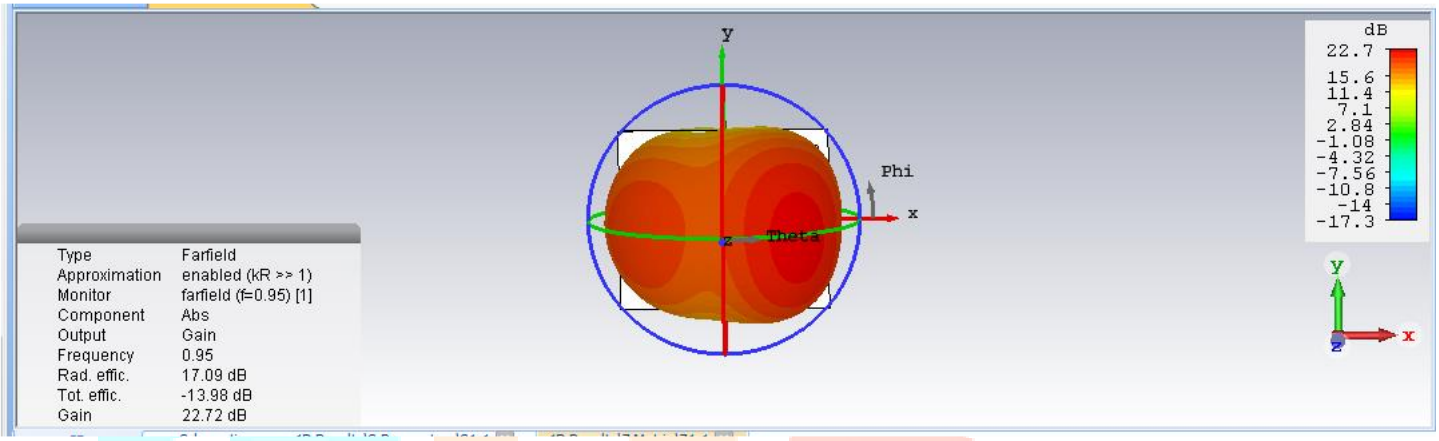

Figure.8: 3 Dimensional view of antenna at 950 MHz.

The proposed antenna is having Gain of 22.72 dB at 950 MHz frequency0000000000

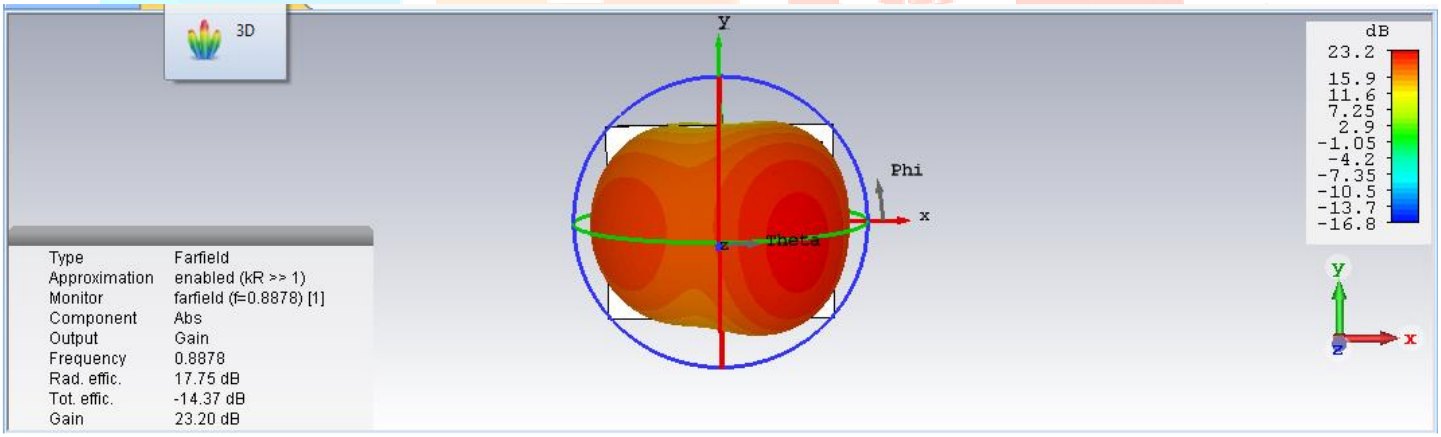

Figure.9: 3 Dimensional view of antenna at 887 MHz.

The proposed antenna is having Gain of 23.20 dB at 887 MHz frequency.

IV. conclusion

This project presents configuration, design theory, simulation, and measurement of a novel UHF RFID reader antenna for near-field applications. The proposed antenna was shown to generate a multipolarized electric field with a fairly uniform distribution in the near-field region in simulation. The performance of the proposed antenna was verified and evaluated by conducting several experimental tests. All the results demonstrate that the proposed antenna can perform well in the specific UHF RFID near-field applications. However, the 100% reading rate area of the proposed antenna has a fixed reading zone, which is not easy to adjust. This limitation can, hopefully, be overcome by further research work in the future.

V. References

[1] R. Want, "An introduction to RFID technology," IEEE Pervasive Comput., vol. 5, no. 1, pp. 25–33, 2006.

[2] J. Landt, "The history of RFID," IEEE Potentials, vol. 24, no. 4, pp. 8–11, Oct. 2005.

[3] K. Finkenzeller, RFID Handbook. Hoboken, NJ, USA: Wiley, 2000.

[4] P. V. Nikitin, K. V. S. Rao, and S. Lazar, "An overview of near field UHF RFID," in Proc. IEEE Int. Conf. RFID, Mar. 2007, pp. 167–174.

[5] K. Jaakkola and P. Koivu, "Low-cost and low-profile near field UHF RFID transponder for tagging batteries and other metal objects," IEEE Trans. Antennas Propag., vol. 63, no. 2, pp. 692–702, Feb. 2015.

[6] T. A. Morgado et al., "Spatially confined UHF RFID detection with a metamaterial grid," IEEE Trans. Antennas Propag., vol. 62, no. 1, pp. 378–384, Jan. 2014.

[7] X. M. Qing, C. K. Goh, and Z. N. Chen, "A broadband UHF nearfield RFID antenna," IEEE Trans. Antennas Propag., vol. 58, no. 12, pp. 3829–3838, Dec. 2010.

[8] J. Shi, X. Qing, Z. N. Chen, and C. K. Goh, "Electrically large dualloop antenna for UHF near-field RFID reader," IEEE Trans. Antennas Propag., vol. 61, no. 3, pp. 1019–1025, Mar. 2013.

[9] J. Shi, X. Qing, and Z. N. Chen, "Electrically large zero-phase-shift line grid-array UHF near-field RFID reader antenna," IEEE Trans. Antennas Propag., vol. 62, no. 4, pp. 2201–2208, Apr. 2014.

[10] J. Hong, J. Choo, J. Ryoo, and C. Choi, "A shelf antenna using nearfield without dead zones in UHF RFID," in Proc. IEEE Int. Conf. Ind. Technol., Feb. 2009, pp. 1–4.

[11] C. R. Medeiros, J. R. Costa, and C. A. Fernandes, "RFID smart shelf with confined detection volume at UHF," IEEE Antennas Wireless Propag. Lett., vol. 7, pp. 773–776, 2008.

[12] T. Lu, Q. Liu, Y. Yang, and X. He, "A simple UHF RFID near-field reader antenna based on micro-stripe transmission line," in Proc. Asia–Pacific Conf. Antennas Propag., Jul. 2014, pp. 193–196.

[13] A. Michel, A. Buffi, R. Caso, P. Nepa, G. Isola, and H. T. Chou, "Design and performance analysis of a planar antenna for near-field UHF-RFID desktop readers," in Proc. Asia–Pacific Microw. Conf., Dec. 2012, pp. 1019–1021.

[14] A. S. Andrenko and M. Kai, "Novel design of UHF RFID near-field antenna for smart shelf applications," in Proc. Asia–Pacific Microw. Conf., Nov. 2013, pp. 242–244.

[15] W. Choi, J. S. Kim, J. H. Bae, G. Choi, and J. S. Chae, "Near-field antenna for RFID smart shelf in UHF," in Proc. IEEE Antennas Propag. Soc. Int. Symp., Jun. 2009, pp. 1–4.

[16] A. S. Andrenko, "Optimized near-field antenna for UHF RFID smart shelf applications," in Proc. IEEE Int. Symp. Antennas Propag. USNC/URSI Nat. Radio Sci. Meeting, Jul. 2015, pp. 1576–1577.

[17] C. Cui, Y. Yao, J. Yu, and X. Chen, "Design of a novel UHF RFID reader antenna for near-field applications," in Proc. IEEE Int. Symp. Antennas Propag. USNC/URSI Nat. Radio Sci. Meeting, Jul. 2015, pp. 1580–1581.

[18] Nasimuddin, Z. N. Chen, and X. Qing, "Asymmetric-circular shaped slotted microstrip antennas for circular polarization and RFID applications," IEEE Trans. Antennas Propag., vol. 58, no. 12, pp. 3821–3828, Dec. 2010.

[19] T. Yamagajo and M. Kai, "A circulary polarized planar antenna for near field and far filed communication systems," in Proc. IEEE Int. Symp. Antennas Propag. USNC/URSI Nat. Radio Sci. Meeting, Jul. 2015, pp. 1570–1571.

[20] T. Yamagajo and M. Kai, "Numerical and experimental study of a novel circularly polarized antenna for near-field and far-field communication systems," in Proc. Eur. Conf. Antennas Propag., Apr. 2016, pp. 1–4.

[21] Speedway RFID Reader Documentation, accessed on Jun. 2016. [Online]. Available: https://support.impinj.com/hc/en-us/articles/202755298-Reader-Documentation

[22] RFID Tags, accessed on Apr. 2016. [Online]. Available: http://www.nationz.com.cn/index.php?ac=article&at=list&tid=2